Hindawi
Mobile Information Systems
Volume 2022, Article ID 5907051, 10 pages
https://doi.org/10.1155/2022/5907051

Research Article

Deformation Prediction and Analysis of Soft Rock Roadway with High Altitude and Large Buried Depth Based on Particle Swarm Optimization LSTM Model

Bin Du, Huahui Yi, and Fan Yang

Xi'an Technology University, Xi'an, Shaanxi 710062, China

Correspondence should be addressed to Bin Du; dubin@xatu.edu.cn

Received 19 July 2022; Revised 16 August 2022; Accepted 23 August 2022; Published 6 September 2022

Academic Editor: R. Mo

Deformation prediction is an important basis for roadway information construction, especially for soft rock roadway at high altitude and large buried depth, whether the deformation of roadway surrounding rock can be effectively and accurately predicted is an important basis for judging the stability of roadway surrounding rock. However, at present, the research on the informatization construction of the roadway is not in-depth, and the intelligent prediction technology for the deformation of the surrounding rock of the roadway is still in its infancy, and the accuracy of deformation prediction is also low. Therefore, based on the research of domestic and foreign researchers, in order to solve the breakthrough of related technology, this paper puts forward the deformation prediction and control technology of high altitude and deep buried soft rock roadway based on a neural network model. This method is based on the traditional prediction model and is replaced by the neural network, so as to improve the problems of low accuracy and large prediction deviation in the related deformation prediction of the traditional prediction model. At the same time, aiming at the problem of poor local weight and network search ability, an improved method using particle swarm optimization algorithm is proposed, which effectively considers the influence of local and global factors on the combined weight. Finally, the improved deformation prediction model of high altitude and deep buried soft rock roadway based on particle swarm optimization LSTM model is applied to an engineering example and compared with the traditional model to explore its feasibility and effectiveness. The results show that the prediction model has higher prediction accuracy than the traditional prediction model, and the relative deviation of the prediction results is controlled within 2%. At the same time, compared with other models (BP neural network model), it has relatively higher accuracy and stability. The research results can provide a new idea for the deformation prediction of soft rock roadway with high altitude and deep burial.

1. Introduction

With the rapid development of China's economy, the demand for energy is increasing. Energy mining, especially coal mining, has entered deep mining from shallow mining. In order to ensure the safety of mine production, how to accurately predict the deformation of surrounding rock of deep roadway and give a reasonable support scheme is particularly important.

At present, with the increase of mining depth of coal mines in various geological environments, affected by geological conditions, it is inevitable to face more and more soft rock problems. Many scholars have done a lot of research on the deformation prediction of deep soft rock roadway, and have also achieved many important research results. The deformation prediction methods of surrounding rock of roadway commonly used in engineering circles [1–3] mainly include theoretical formula calculation method, experimental method, engineering experience method, numerical simulation method, neural network deformation prediction method, and so on.

Although the theoretical calculation method can get a more accurate analytical solution, it must assume harsh preconditions in the calculation process, and can only solve relatively simple mechanical models. For underground engineering, the geological environment of rock mass is complex, and the layout and section size of roadway are complex, which is generally difficult to be solved by theoretical calculation method [4–6]. Experimental methods generally include indoor test and in-situ test. When carrying out the indoor test of samples, due to the damage caused by the sampling process to the influence of stress disturbance and size effect, the obtained rock mass mechanical parameters are much different from the actual rock mass mechanical parameters [7]. On the other hand, because the rock mass is a heterogeneous structure, the rock mass is divided by different joints and fissures, and the joints and fissures are filled with different substances, resulting in the extremely uneven stress of the rock mass and the complex geological environment structure of the rock mass, which makes the rock mass in different parts have great discreteness. It is difficult to comprehensively reflect the mechanical parameters of rock mass through field tests, and the mathematical model thus established is more difficult to reflect the real deformation, and the deformation prediction thus obtained is more difficult to achieve high prediction accuracy [8–11]. Because the rock masses of different strata and different sections are very different, the role of the engineering experience method in different engineering environments can be ignored. For underground engineering, the numerical calculation method [12–15] has obvious advantages over other methods. It can calculate most underground engineering problems, with wide applicability, fast calculation speed, and low cost. However, during the modeling of numerical simulation, due to the difficulty of obtaining parameters, the numerical model thus constructed is also difficult to reflect the real situation. The natural accuracy of roadway prediction is also difficult to meet people's expectations.

As a new deformation prediction technology developed in recent years, the neural network prediction method, due to its strong nonlinear processing ability [16–19], when predicting the deformation of roadway surrounding rock, does not need to assume harsh preconditions like the theoretical method, nor many parameters like the numerical simulation method, but only some basic parameters and data to realize the accurate prediction of surrounding rock, and gradually liked by people [4, 20–23]. At present, the artificial neural network model has been widely used in various fields of engineering, and the prediction accuracy of surrounding rock deformation of relevant tunnels has also been improved year by year, but there is still a large research space [3, 24, 25].

In view of the above problems, in order to explore the deformation law of soft surrounding rock under the geological conditions of high altitude and large buried depth and accurately predict it, this paper, based on the large buried deep soft rock roadway in a high altitude area in China, uses neural network and field monitoring methods to carry out the deformation prediction research of large buried deep soft surrounding rock roadway in high altitude area, so as to provide a reference for the design of similar high altitude and large buried deep soft surrounding rock roadway provide a reference for construction and deformation prediction.

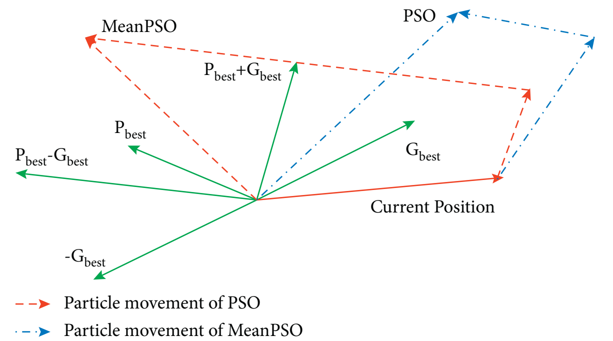

Figure 1: MeanPSO algorithm and particle evolution process of PSO algorithm.

2. Overview of Particle Swarm Optimization Algorithm and Human Long-Term and Short-Term Memory Neural Network

2.1. General PSO. PSO algorithm is a search method based on group cooperation, which is generated by simulating birds seeking the optimal route when foraging [26–28]. In PSO algorithm, there is a particle space, in which each particle has its own initial position and initial velocity, forming a d-dimensional space with m particles. Through continuous iteration, the speed and position of particles are constantly updated to form local optimal solutions and global optimal solutions.

In ordinary PSO algorithm, particles search for the optimal particle by learning their own historical experience (P_{best}) and group experience (G_{best}). For the optimization problem with variable $X = (x_1, x_2, \cdots, x_D)$ and objective function $\min\{f(x)\}$, the particle update formula of the standard PSO algorithm is formulas (1) and (2)

$$v_{id}(t+1) = wv_{id}(t) + c_1 r_1 \left(P_{best_{id}} - x_{id}(t)\right) + c_2 r_2 \left(G_{best_{id}} - x_{id}(t)\right), \tag{1}$$

$$x_{id}(t+1) = x_{id}(t) + v_{id}(t+1), \tag{2}$$

where $v_{id}(t+1)$ stands for speed and $x_{id}(t+1)$ are stands for position, w stands for the weight, and w in ordinary PSO decreases with the number of iterations.

2.2. Improved PSO Algorithm. Through the above analysis, it can be found that for the ordinary PSO algorithm, its speed and position update of particles are relatively common in the path exploration of particles, which is often difficult to meet the needs of practical projects. In the face of complex data, it has great limitations. Therefore, aiming at the above problems, this section focuses on the improvement of particle speed and position update. The specific improvement process includes the following two points.

2.2.1. Improvement of Particle Velocity Update Formula. Reference [27] proposes a mean particle swarm optimization (MeanPSO) algorithm, which uses the linear combination $P_{best_{id}} + G_{best_{id}}/2$ and $P_{best_{id}} - G_{best_{id}}/2$ of individual optimization and group optimization to replace $P_{best_{id}}$ and $G_{best_{id}}$ in formula (1), respectively, and obtains a new particle velocity update formula, which is formula (3)

$$v_{id}(t+1) = wv_{id}(t) + c_1 r_1\left(\frac{P_{best_{id}} + G_{best_{id}}}{2} - x_{id}(t)\right) + c_2 r_2\left(\frac{P_{best_{id}} - G_{best_{id}}}{2} - x_{id}(t)\right). \quad (3)$$

The particle motion process in MeanPSO algorithm and PSO algorithm is shown in Picture. From Figure 1, it can be seen that the particle search interval in meanpso algorithm is wider, which makes the algorithm more likely to search for the global optimal solution in the early stage of evolution.

2.2.2. Improvement of Particle Position Update Formula. Reference [29] proposes a hierarchical simplified PSO algorithm with average dimension information. Phspo algorithm discards the particle velocity update item in PSO algorithm and introduces the concept of average dimension information, that is, the average value of all dimensional information of each particle, and the calculation formula is formula (4). At the same time, PHPSO algorithm decomposes the particle position update formula into three modes, They are equations (5)–(7), respectively.

$$P_{ad}(t) = \frac{1}{D}\sum_{i=1}^{D} x_{id}(t), \quad (4)$$

$$x_{id}(t+1) = wx_{id}(t) + c_1 r_1\left(P_{best_{id}} - x_{id}(t)\right), \quad (5)$$

$$x_{id}(t+1) = wx_{id}(t) + c_2 r_2\left(G_{best_{id}} - x_{id}(t)\right), \quad (6)$$

$$x_{id}(t+1) = wx_{id}(t) + c_3 r_3\left(P_{ad} - x_{id}(t)\right). \quad (7)$$

Among them, equation (5) is conducive to the global development ability of the algorithm; equation (6) is conducive to the local exploration ability of the algorithm, to helps the algorithm jump out of the local optimization; equation (7) helps to improve the convergence speed of the algorithm. In the iterative process, the algorithm selects different modes based on probability to update the particle position.

Reference [26] points out that using "$X = X + V$" to update the particle position helps to improve the local exploration ability of the algorithm, and "$X = wX + (1 - w)V$" helps to Polish up the global development ability of them. This paper proposes an adaptive particle position update mechanism, as shown in equations (8) and (9)

$$P_i = \frac{\exp\left(fitt\left(x_i(t)\right)\right)}{\exp\left(1/N \sum_{i=1}^{N} fit\left(x_i(t)\right)\right)}, \quad (8)$$

$$x_{id}(t+1) = \begin{cases} wx_{id}(t) + (1-w)v_{id}(t+1), & p_i > rand \\ x_{id}(t) + v_{id}(t+1), & else \end{cases}, \quad (9)$$

where $fit(\cdot)$ stands for the fitness value of particles, and N stands for the number of particles in the population. In equation (8), p_i stands for the ratio of the current particle fitness value to the average fitness value of all particles in the population.

Combined with the improved optimization strategy of particles for particle speed and position, a new adaptive particle speed and position update strategy can be obtained, and its update method and process are shown in equations (10) and (11)

$$\begin{cases} v_{id}(t+1) = wv_{id}(t) + c_1 r_1\left(\dfrac{P_{best_{id}} + G_{best_{id}}}{2} - x_{id}(t)\right), \\ +c_2 r_2\left(\dfrac{P_{best_{id}} - G_{best_{id}}}{2} - x_{id}(t)\right), \\ x_{id}(t+1) = wx_{id}(t) + (1-w)v_{id}(t+1), \end{cases} \quad (10)$$

$$\begin{cases} v_{id}(t+1) = wv_{id}(t) + c_1 r_1\left(p_{ad} - x_{id}(t)\right), \\ +c_2 r_2\left(G_{best_{id}} - x_{id}(t)\right), \\ x_{id}(t+1) = x_{id}(t) + v_{id}(t+1). \end{cases} \quad (11)$$

The above adaptive strategy refers to p_i in literature [27–30] as the adaptive judgment condition. When $p_i > \delta$, the fitness value of the current particle is much larger than the average fitness value of all particles in the population, indicating that the algorithm is in the initial stage of search or the current particle distribution is relatively scattered. At this time, equation (10) should update the particle speed and to update the position. Equation (10) introduces a linear combination of individual optimization and population optimization into the speed update term, and the location update adopts "$X = wX + (1 - w)V$" to improve the global search ability of the algorithm; When $p_i < \delta$, there is little difference between the fitness value of the current particle and the average fitness value of all particles in the population, indicating that the algorithm is in the middle and late stage of search or the current particle distribution is relatively concentrated. At this time, equation (11) should be used to update the particle speed and position. In equation (11), position update uses "$X = X + V$" to ensure the local exploration ability of the algorithm and prevent the algorithm from falling into local optimization when solving complex multimodal functions.

In PSO algorithm, w is particularly important. It is of great help to the global and local development of this algorithm. In an ordinary PSO, the linear decreasing method is generally used to change w. Within a certain range, this method has a positive effect on it, but when the data becomes very nonlinear and more complex, this method has little effect. Therefore, we need to find a better way to update the weight.

Heavy nonlinear adjustment strategy. This paper adopts the nonlinear change inertia weight w based on the logistic chaotic map proposed in reference [28, 31]. As a nonlinear map, chaotic map is widely used in evolutionary computation because its chaotic sequence has good randomness and spatial ergodicity. Among them, logistic map is widely used, which can produce [0, 1). Equation (12) gives the definition of logistic mapping, and the definition of w is as shown in equation (13).

$$r(t+1) = 4r(t)(1-r(t)), r(0) = rand, \tag{12}$$

$$w(t) = r(t)w_{\min} + \frac{(w_{\max} - w_{\min})t}{T_{\max}}, \tag{13}$$

where $r(t)$ is the random number generated by the iteration of equation (12). The change of inertia weight is shown in Figure 2.

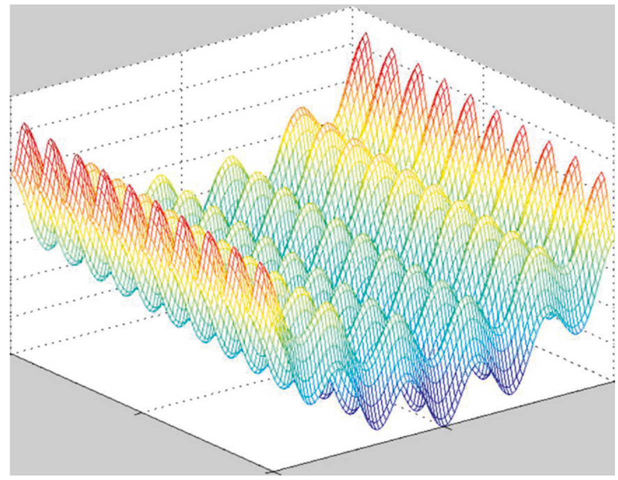

Figure 2: Variation diagram of inertia weight with iteration times.

2.3. LSTM. LSTM neural network was proposed by Hochreiter and Schmidhuber in 1997. It can measure itself and effectively make up for the shortcomings of recurrent neural network (RNN). Compared with RNN, LSTM adds memory units, including forgetting gate, updating gate, and output gate, which can use historical information. LSTM memory unit has long-term and short-term memory mechanism, which is suitable for processing data sequences with certain time intervals. The unit structure of LSTM neural network is shown in Figure 3. It mainly includes three "gate" structures and memory cells. The function of the forgetting gate is to decide which information should be discarded or retained, which determines the cell state c at the last time_ How much $t-1$ is reserved to the current time c_t; the input gate is used to update the status, which determines the input x of the network at the current time_t how much is saved to the unit state c_t; the output gate is used to determine the value of the next hidden state, control unit state c_t how many outputs are there to the current output value of LSTM h_t. The key to understanding short-term and long-term memory neural networks is the rectangular box below, which is called memory block.

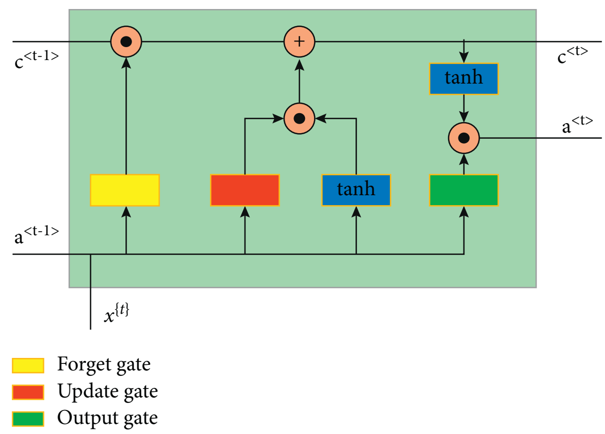

Figure 3: LSTM structure diagram.

3. Construction of Tunnel Deformation Prediction Model of PSO-LSTM

In order to improve the prediction accuracy of surrounding rock deformation of deep buried soft rock roadway in high altitude areas, and make full use of the advantages of a single model, PSO and LSTM neural networks are applied to the prediction of surrounding rock deformation of deep buried soft rock roadway in high altitude area, and a pso-lstm combined model is constructed. The combined model is divided into four stages: data acquisition and processing, PSO optimization, deformation prediction, and prediction result analysis and evaluation.

(1) The first stage is the data preprocessing stage, which refers to the component analysis and dimensionless processing of the surrounding rock deformation data of the deep buried soft rock roadway in the high altitude area by using a series of methods such as principal component analysis, so as to obtain the model input parameters and data;

(2) The second stage is the PSO optimization stage, which refers to using the data processed in the first stage to input the LSTM model, and then using PSO to determine the iteration times, learning rate, and the number of neurons in the hidden layer of the LSTM neural network;

(3) The third stage is the deformation prediction stage, which is also divided into two steps. The first step is the training of the model, that is, the on-site measured data of the roadway are classified by algorithm, one for model training and one for model testing. In this paper, the training data and test data are randomly divided according to 7 : 3;

(4) The fourth stage, the last stage of the model, is the result analysis of the data. By the above steps, the

deformation prediction of the surrounding rock of the deep buried soft rock roadway in the high altitude area is realized, and the final prediction result is obtained. Through the selection of the model evaluation index, the error analysis is carried out.

3.1. Data Acquisition and Processing Stage

3.1.1. Roadway Deformation Data Acquisition. The data set used in this study is from the actual roadway measurement. The data set from each roadway location is analyzed separately, and then those discrete and unreliable data are removed from the data set. Finally, a total of 100 data (measured in a roadway) are selected to develop the pso-lstm deformation prediction model and trial and error training model constructed in this paper. These data sets include the rock mass deformation modulus obtained by the bearing plate method, the rock mass deformation modulus (EM), uniaxial compressive strength (UCS), rock mass quality index (RQD), dry density, the number of joints per unit length (*J*), and porosity of the complete rock obtained by using a core with a diameter of 40 mm. All parameter data collected in this paper are shown in Table 1.

3.1.2. Data Preprocessing. In many neural network algorithms, it is assumed that the variance of each variable is of the same order. If the variance of a certain factor is particularly large, for example, the basic surrounding rock parameter value of the roadway is several times the surrounding rock density, then this feature will dominate the algorithm. It is difficult for the model to learn rules from features with small orders of magnitude. In order to solve this problem, we map the original data to the specified interval according to certain change rules. The scaling of this data set is data normalization. After standardization, the original data are transformed into dimensionless values on the interval, which facilitates the weighting and comparison of indicators with different units and orders of magnitude. In this paper, min-max standardization method is mainly used for data preprocessing. This method is to linearly change the initial data to 0 to 1, and the conversion function is shown in the following formula:

$$x' = \frac{x - \min A}{\max A - \min A}. \tag{14}$$

3.1.3. Data Feature Selection. For the deformation data of roadway surrounding rock, although through our efforts, we have screened the above six related quantities from dozens of original data. However, not all these variables are independent of each other. Therefore, we can choose some methods to simplify and reduce the dimension of variables with weak attribute significance or factors with high correlation. Pearson correlation coefficient is often used in the processing of engineering data because of its simple operation method and the universality of applicable conditions. It is also the most commonly used linear correlation coefficient at present.

$$\rho_{x,y} = \frac{\operatorname{cov}(X,Y)}{\sigma_X \sigma_Y} = \frac{E[(X-\mu x)(Y-\mu y)]}{\sigma_X \sigma_Y}, \tag{15}$$

where Cov (X, Y) represents the covariance of the above parameters and σ_X and σ_Y represents the variance of the above parameters.

The correlation between these factors is shown in Figure 4.

In the above thermodynamic diagram, if the correlation between 0 and 0.2 represents no correlation or very weak correlation between the two variables, between 0.2 and 0.4 represents weak correlation between the two variables, between 0.4 and 0.6 represents medium correlation between the two variables, between 0.6 and 0.8 represents strong correlation between the two variables, and between 0.8 and 1 represents very strong correlation between the two factors, it can be seen that the correlation of the above factors for roadway deformation is above 0.6, so when making model prediction input, All variables should be input variables.

3.2. PSO Optimization. The detailed steps of optimizing LSTM using PSO are as follows: (1) initialize particle swarm parameters. Determine the size of the population, the number of iterations, learning factors, search dimensions, and the value range of location and speed. (2) Initialize the position and speed of particles. A particle is randomly generated, $X_i = (n, lr, h_1, h_2)$, n is the number of iterations of LSTM, lr is the learning rate, $h1$ is the number of neurons in the first hidden layer, and $H2$ is the number of neurons in the second hidden layer. The velocity $V_i = (V_{i1}, V_{i2}, V_{i3}, V_{i4})$ of particles produces a set of random sample values with uniform distribution of 0~1. The range of random samples is [0, 1). (3) Determine other parameters of LSTM. Determine the prediction scheme as one-step prediction, that is, use the data of the previous r historical periods $\{x_1, x_2, \cdots, x_n\}$ to predict the data of the next time period x_{n+1}; r value is 10. (4) Determine the fitness function of PSO algorithm. Construct LSTM with initialized particle swarm parameters, and take the mean square error between the measured value and the predicted value of the training set as the fitness function $f(r)$ of particle swarm. $f(r) = 1/N \sum (x_r - \hat{x}_r)^2$, x_r is the measured value of passenger flow, $\hat{x}_r$ is the passenger flow N is the total length of time to be predicted, $n = 210$. (5) Calculate the position of particles in each iteration and calculate the fitness value. By comparing with the fitness value of the initial position, the individual optimal position $P_{i\text{best}}$ is determined, and then the group optimal position $P_{g\text{best}}$ is determined. According to formulas (5) and (6), constantly adjust the position and speed of particles until the fitness function is minimum, and determine the optimal position, that is, determine the optimal parameters of LSTM, so as to build PSO-LSTM model.

3.3. Tunnel Deformation Prediction. PSO-LSTM model is used to predict the deformation data of roadway

Table 1: Statistical description of extracted rock mass attributes.

Data type	E_m (GPa)	UCS (MPa)	GSI	RQD (%)	Density (kg/m^3)	Porosity (%)
Average value	9.8	88.4	36.8	55.2	2.43	5.5
Standard error	0.56	2.4	0.49	0.94	0.02	0.24
Median	8.4	113.4	37.2	44.5	2.47	3.97
Sample variance	51.2	1562.7	57.8	402.3	0.09	10.2
Minimum value	2.3	7.4	16.4	12.4	2.16	0.15
Maximum value	17.5	102.6	46.8	97.5	2.51	13.5

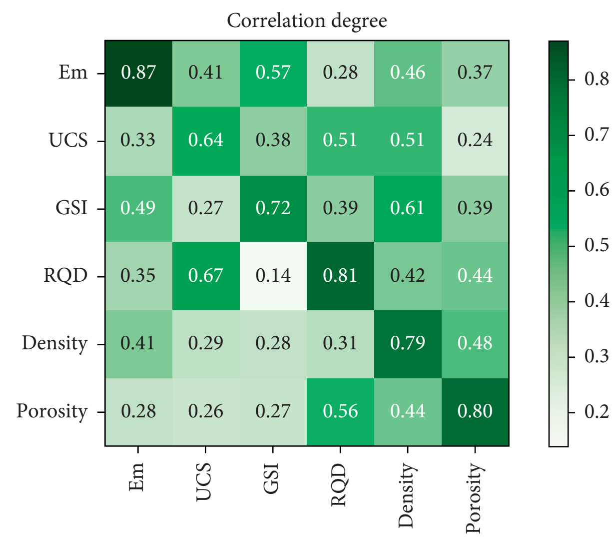

Figure 4: Thermodynamic diagram of correlation among factors.

surrounding rock, and the final prediction result is obtained. The short-term passenger flow prediction process of pso-lstm combined model is shown in Figure 5.

3.4. Prediction Result Analysis and Evaluation Stage. The R^2 value is used as the evaluation index to judge the accuracy of the deformation prediction model of deep buried soft rock roadway in high-altitude areas. The calculation formula of each evaluation index is as follows:

$$R^2 = 1 - \frac{\sum_{i=1}^{m} \left(h\left(x_i\right) - y_i\right)^2}{\sum_{i=1}^{m} \left(\mathrm{y_i} - \overline{y}\right)^2}. \qquad (16)$$

In the determination coefficient expression, the denominator is the dispersion degree of the original data, that is, the total sum of squares, and the numerator is the error between the true value and the estimated value, that is, the regression square. The interference caused by data dispersion is eliminated by dividing these two parameters, which reflects the goodness of fit of the model. The value range of the determination coefficient is 0 to 1. The larger the value of the determination coefficient (close to 1), the better the simulation effect; mean absolute error is usually used to evaluate the degree of change of data, and it is also used as the loss function of linear regression; the smaller the value, the more accurate the model description; root mean square error is a measure of the deviation between the observed value and the real value. Compared with RMSE, it uses the

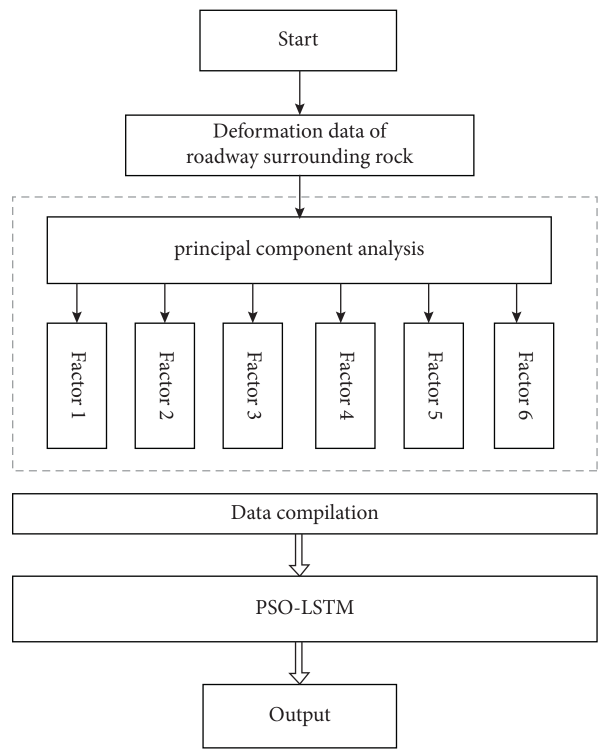

Figure 5: Short term passenger flow prediction process of PSO-LSTM combined model.

most reliable value to replace n in the actual data, eliminating the sensitivity of extremely small and extra large values in the mean square error.

4. Engineering Examples and Result Analysis

4.1. Project Overview. In order to verify the reliability of pso-lstm model in engineering practice, this study selects the large deformation data of the excavated section of a coal mine deep roadway project as the learning sample. The structure of the 3# coal seam studied is relatively complex, and the thickness is generally in the range of 3.5~6.2 m, with an average thickness of 5.5 m. The burial depth is basically 463.9 m~633.9 m, with an average of 500 m. The coal seam structure can be mainly summarized into linear banded and layered structures. The joints of the coal seam are relatively developed and complex. The joint density of the coal seam in a specific direction is relatively large. The joint surface is generally not straight, the cracks are tight, and there is no filling. The joints in other directions extend relatively short, the joint surface is not straight enough, and the development

Table 2: Geological conditions of the stratum where the roadway is located.

Cumulative thickness (m)	Layer thickness (m)	Rock name and lithology description
517.6–525.4	7.8	The rock is gray, broken, and semi-hard
525.4–530.5	5.1	Carbonaceous mudstone, thin-layer, rich in plant-based fossils
530.5–541.3	10.8	Black, mainly bright coal, carbonaceous mudstone
541.3–544.9	3.6	The rocks are relatively complete and contain plant fossils
544.9–561.7	16.8	Black mudstone, semi-hard, horizontal texture

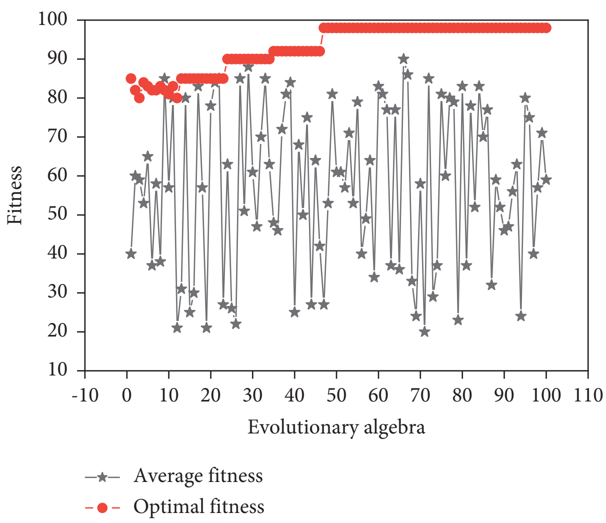

Figure 6: PSO finding the fitness curve of the best parameters.

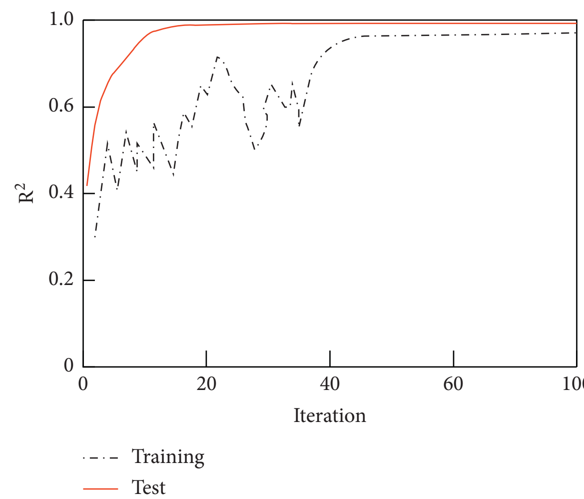

Figure 7: PSO-LSTM model training and testing R^2 value change curve.

density and standardization are not strong. During the excavation process, it is revealed that the cracks of the coal seam and roof rock are developed, and the roof is broken, which is easy to collapse and collapse, coal seams are very easy to chip. The maximum horizontal principal stress in the mining area is in the range of 10~15 MPa, mainly structural stress. The maximum horizontal principal stress is 14.83 MPa, the vertical principal stress is 12.63 MPa, and the minimum horizontal principal stress is 8.12 MPa. The roof strata of the coal roadway are mainly sandy mudstone, then siltstone and local strata are distributed with medium-grained sandstone and fine-grained sandstone. The roadway floor strata are mainly mudstone and sandy mudstone, and the distribution range of medium-sized sandstone, fine-grained sandstone, or siltstone is less. The geological conditions of the mining area where the studied coal seam roadway is located are shown in Table 2.

4.2. Establishment and Training of Improved pso-lstm Large Deformation Prediction Model. The six evaluation indexes of the obtained 100 groups of learning samples are divided into three parts after the pretreatment shown above. The pso-lstm model is trained with 2/3 learning samples. After the training, the reserved 1/3 samples are identified one by one. The parameters of the PSO algorithm are set as: acceleration $c_1 = 1.5$, $c_2 = 1.7$, termination algebra 100, and population number $p = 20$. After multiple iterations, the optimal values of LSTM parameters $c = 12$, $g = 0.31$ are obtained. The change process of parameter optimization fitness is shown in Figure 6. It can be seen from Figure 6 that the model achieves global optimization in 47 iterations.

The variation curve of R^2 value in pso-lstm model training and testing is shown in Figure 7. It can be found from the variation curve of R^2 value of pso-lstm model training and testing in Figure 7 that during the training of this model, due to the different properties of roadway surrounding rock, the fluctuation during the training is large, and the fitting degree of the data is not high. However, when the training times exceed a certain number, the R^2 value of the model tends to be stable, and always remains around 0.95; during the test, because the model is familiar with the deformation law of roadway surrounding rock, it shows good performance and degree in the test. The R^2 value tends to be stable after many times of crossing, close to 1.0, up to 0.9786, indicating that the prediction accuracy of the model for the deformation of roadway surrounding rock is high.

In addition to evaluating the accuracy of the models built in the article, we also need to compare and analyze the models. Therefore, this paper also selects two prediction models commonly used in our prediction research in the engineering field, BP and conventional LSTM, which have prominent advantages and have been well applied in various engineering fields. Similarly, in the comparative analysis, we also use R^2 value as the evaluation result of the comparative analysis model. Through modeling and putting the same data into the training test, it can be found that, different from the prediction model constructed in the above article, when comparing model 1, that is, BP model is used to predict the

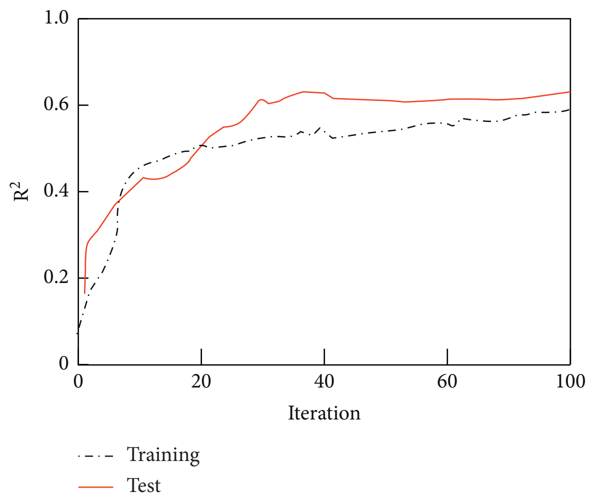

Figure 8: BP model training and testing R^2 value change curve.

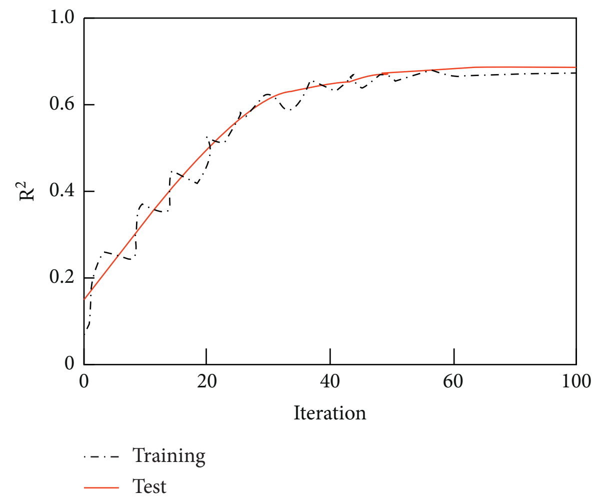

Figure 9: LSTM model training and testing R^2 value change curve.

deformation of the roadway, due to the limitation of the model itself on the processing ability of complex data, the initial value and degree of the model are low, and its initial value and degree of training are less than 0.1, which can be said to be basically not fitted, although with the increase of the number of iterations, The final fitting degree is no more than 0.65, and the maximum fitting degree is only 0.616. Therefore, the prediction accuracy of the roadway deformation comparison model 1 established in this paper is far lower than that of the model established in this paper; Similarly, for comparison model 2, LSTM, this model shows a better fitting curve than comparison model 1. The fitting degree of the test curve is also close to that of the training curve, and the two are always consistent. At the same time, its prediction accuracy is higher than the former model, and the maximum fitting degree is as high as 0.863. However, there are also similar problems with comparison model 1. First, the initial accuracy of the model is not enough, In addition, the convergence speed of the model is also slow, which is difficult to meet the actual work needs for some problems that need rapid prediction.

Based on the training and testing R2 value change curves of the three different models in Figures 7–9, it is found that, first, in the case of small sample size, compared with BP and LSTM models, pso-lstm model has higher prediction accuracy for the deformation of roadway surrounding rock, which proves that the improved pso-lstm combined prediction model constructed in this paper has a good training effect for small samples, which has a good applicability to some projects under complex environmental conditions. Second, from the perspective of the convergence of the model, the model constructed in this paper is obviously superior to the comparison model in terms of convergence speed, and the convergence curve shown by the model is also more in line with the actual process, which can eliminate the overfitting and under fitting phenomena in the process of model training, while the comparison model 2 may have overfitting phenomena. At the same time, this rapid convergence ability is very important for this high altitude, large burial depth The rapid deformation prediction of the complex geology of weak surrounding rock is very helpful. Finally, through comprehensive comparison, it is found that the model constructed in this paper is superior to other comparison models in terms of initial prediction accuracy and convergence. Its time required is shorter and the overall effect is better. It can be judged that the deformation prediction model of LSTM based on PSO optimization constructed in this paper has the advantages of higher accuracy and better generalization of large deformation prediction.

5. Conclusion

With the continuous increase of coal mining depth, the mining depth of many mines has reached thousands of meters, and the rocks show certain rheological properties. Especially for highaltitude areas, under the action of high ground stress, the ground pressure of soft rock roadway shows intense and large deformation, and the support problem of deep buried high-stress soft rock roadway is becoming more and more prominent. Therefore, studying the deformation prediction technology of deep buried soft rock roadway is of great significance to control the stability of roadway surrounding rock. In order to solve the above problems, this study proposes a PSO-LSTM large deformation prediction method for layered soft rock tunnels based on in-situ stress inversion and on-site large deformation monitoring information through machine learning method, which provides a new research idea for hierarchical prediction of large deformation of layered soft rock tunnels. At the same time, the related models are optimized to improve the prediction accuracy, and the feasibility of this method is verified by engineering application, and the following conclusions are obtained.

(1) Through the field monitoring data, it is found that the influencing factors of large deformation of layered soft rock tunnels are complex and changeable. Taking full account of the anisotropy of layered soft

rock, six evaluation indexes for large deformation prediction are selected. The large deformation data of the excavated section of the target tunnel and the field measurement information are used as the learning samples of machine learning, which is more true and accurate than the learning samples obtained from other tunnels.

(2) Using the on-site monitoring technology and combined neural network modeling technology, a combined neural network deformation prediction model of high altitude and deep buried soft rock roadway based on PSO and LSTM is constructed. Through the model training, it is found that the PSO improved by this paper on particle velocity and updating method has more advantages than the traditional PSO.

(3) Through practice, BP, LSTM, and pso-lstmm are used to predict the same sample data. The results show that the accuracy of the test set of pso-lstm model for large deformation prediction is as high as 97.86%, and its prediction results and speed are better than BP and LSTM models.

Data Availability

The data used to support the findings of this study are available from the corresponding author upon request.

Conflicts of Interest

The author declares that there are no conflicts of interest.

References

[1] Y. U. Wei-Jian, Y. Yuan, and W. J. Wang, "Deformation mechanism of roadway surrounding rock with large deformation and control technology under difficult conditions," *Coal Science and Technology*, 2015.

[2] J. Wang, M. Lin, D. Tian, and Cl Zhao, "Deformation characteristics of surrounding rock of broken and soft rock roadway," *Mining Science and Technology*, vol. 19, no. 2, pp. 205–209, 2009.

[3] C. Q. Zhu, T. Feng, and S. L. Shi, "Application of neural network in optimal selection of bolt support patterns and deformation prediction of extraction roadway in fully-mechanized caving face," *Journal of China Coal Society*, 2005.

[4] Q. Xu, Y. Li, J. Lu, and L. Zhang, "The use of surrounding rock loosening circle theory combined with elastic-plastic mechanics calculation method and depth learning in roadway support," *PLoS One*, vol. 15, no. 7, Article ID e0234071, 2020.

[5] U. C. Han, C. S. Choe, K. U. Hong, and C. Pak, "Prediction of final displacement of tunnels in time-dependent rock mass based on the nonequidistant grey verhulst model," *Mathematical Problems in Engineering*, vol. 2022, Article ID 3241171, 11 pages, 2022.

[6] H. Zhang, X. Miao, G. Zhang, Y. Wu, and Y. Chen, "Non-destructive testing and pre-warning analysis on the quality of bolt support in deep roadways of mining districts," *International Journal of Mining Science and Technology*, vol. 27, no. 6, pp. 989–998, 2017.

[7] B. Meng, H. Jing, K. Chen, and H. Su, "Failure mechanism and stability control of a large section of very soft roadway surrounding rock shear slip," *International Journal of Mining Science and Technology*, vol. 23, no. 1, pp. 127–134, 2013.

[8] G. F. Zhang, K. H. Zeng, and C. Zhang, "Failure mechanism and support design of interclated roadway surrounding inclined coal seam in Qishan coal mine," *Journal of Mining & Safety Engineering*, vol. 28, no. 1, pp. 22–27, 2011.

[9] X. H. Cui, Y. F. Gao, and Q. Z. Fan, "Optimum calculating method for constant resistant supporting of roadway surrounding rock," *Chinese Journal of Geotechnical Engineering*, vol. 12, no. 1, 2006.

[10] C. Zhao, Y. Li, G. Liu, and X. Meng, "Mechanism analysis and control technology of surrounding rock failure in deep soft rock roadway," *Engineering Failure Analysis*, vol. 115, Article ID 104611, 2020.

[11] L. Wang and G. Zhao, "Analysis of instability mechanism and support technology of surrounding rock in high stress soft rock mining roadway," *Iop Conference*, vol. 199, 2018.

[12] M. A. Abido, "Optimal des'ign of power system stabilizers using particle swarm opt'imization," *IEEE Power Engineering Review*, vol. 22, no. 7, p. 53, 2002.

[13] F. Zeng, C. Zou, and L. T. University, "Numerical simulation of roadway surrounding rock deformation and destruction," *Journal of Liaoning Technical University*, vol. 32, no. 12, 2013.

[14] J. Jiang, G. Qin, and C. Liu, "Dynamic feature study of fully-mechanized caving roadway surrounding rock system," *Chinese Journal of Rock Mechanics and Engineering*, vol. 25, no. 9, pp. 1755–1764, 2006.

[15] Y. F. Xun, "Analysis on affects of in-situ horizontal stress to stability of rock surrounding roadway," *Journal of China Coal Society*, vol. 35, no. 6, pp. 891–895, 2010.

[16] Y. H. Shi and Z. Y. He, "New neural network for pattern recognition," *Electronics Letters*, vol. 27, no. 15, pp. 1353–1355, 1991.

[17] X. Du and J. Yu, "Graph neural network-based early bearing fault detection," 2022.

[18] L. Wei, S. Xv, and B. Li, "Short-term wind power prediction using an improved grey wolf optimization algorithm with back-propagation neural network," *Clean Energy*, vol. 6, no. 2, pp. 288–296, 2022.

[19] M. Anthony and P. L. Bartlett, "Neural network learning: theoretical foundations," *AI Magazine*, vol. 22, no. 2, pp. 99-100, 1999.

[20] H. Chen and R. Wang, "Artificial neural network's application in intelligent displacement back analysis of deep mine roadway surrounding rock," in *Proceedings of the 2010 International Conference on Intelligent Computation Technology and Automation*, Changsha, China, May 2010.

[21] None, B. Conference, An artificial neural network for forecasting the amount of Chinese colliery roadway surrounding rock deformation: yuxiang Zhang & 6 others Applications of computers and operations research in the minerals industries," *International Journal of Rock Mechanics & Mining ences & Geomechanics Abstracts*, vol. 33, no. 5, p. A232, 1996.

[22] Y. Shen and A. Zhang, "The stability classification system of roadway surrounding rock based on VC++ 6.0 and BP neural networks," in *Proceedings of the International Symposium on Electronic Commerc*, Guangzhou, China, August 2010.

[23] H. E. Wei, M. Hong, and X. Meng, "Inversion of rheological parameters of surrounding rocks in a mine roadway based on

BP neural network," *Journal of Mines, Metals and Fuels*, vol. 65, no. 3, pp. 149–155, 2017.

[24] S. Yu, H. Zhang, and Y. Chang, "Application of GRNN in time series prediction for deformation of surrounding rocks in soft rock roadway," in *Proceedings of the 2011 Fourth International Conference on Intelligent Computation Technology and Automation*, IEEE, Shenzhen, China, March 2011.

[25] B. Tan, H. Zhang, and G. Cheng, "Constructing a gas explosion inversion model in a straight roadway using GA-BP neural network," 2021.

[26] G. C. Chen and Y. U. Jin-Shou, "Particle SWARM OPTIMIZATION ALGorithm," *Information and Control*, vol. 186, no. 3, pp. 454–458, 2005.

[27] R. C. Eberhart, "Comparing inertia weights and constriction factors in particle swarm optimization," in *Proceedings of the 2000 IEEE Congress on Evolutionary Computation*, IEEE, La Jolla, CA, 2002.

[28] Y. H. Shi and R. C. Eberhart, "Empirical study of particle swarm optimization," in *Proceedings of the Congress on Evolutionary Computation*, IEEE, Prague, Czech Republic, July 2002.

[29] J. Robinson and Y. Rahmat-Samii, "Particle swarm optimization in electromagnetics," *IEEE Transactions on Antennas and Propagation*, vol. 52, no. 2, pp. 397–407, 2004.

[30] M. Clerc and J. Kennedy, "The particle swarm - explosion, stability, and convergence in a multidimensional complex space," *IEEE Transactions on Evolutionary Computation*, vol. 6, no. 1, pp. 58–73, 2002.

[31] S. W. Lin, K. C. Ying, S. C. Chen, and Z. J. Lee, "Particle swarm optimization for parameter determination and feature selection of support vector machines," *Expert Systems with Applications*, vol. 35, no. 4, pp. 1817–1824, 2008.